

# Aromatic Borozone

N. Gonzalez Szwacki · V. Weber · C. J. Tymczak

Received: 13 May 2009 / Accepted: 26 May 2009 / Published online: 11 June 2009  
© to the authors 2009

**Abstract** Based on our comprehensive theoretical investigation and known experimental results for small boron clusters, we predict the existence of a novel aromatic inorganic molecule,  $B_{12}H_6$ . This molecule, which we refer to as *borozone*, has remarkably similar properties to the well-known benzene. Borozone is planar, possesses a large first excitation energy,  $D_{3h}$  symmetry, and more importantly is aromatic. Furthermore, the calculated anisotropy of the magnetic susceptibility of borozone is three times larger in absolute value than for benzene. Finally, we show that borozone molecules may be fused together to give larger aromatic compounds with even larger anisotropic susceptibilities.

**Keywords** Aromatic · Boron · Boron hydrides · Ab initio · FreeON · NICS · Planar molecules

## Introduction

Why certain molecules are more stable than others is not always easy to understand. Nature's diversity does not always permit a simple answer for the structure of all compounds. However, a very useful concept in structural stability is aromaticity [1, 2], which was first developed to account for the properties of organic compounds involving

ring structures such as benzene ( $C_6H_6$ ) and more recently extended to inorganic systems [3]. However, the question arises whether aromatic hydrocarbons are the only structures where an “aromatic ring” acts as a building block and plays a key role in their stability. In this study, we predict the existence of a novel inorganic molecule,  $B_{12}H_6$ , that has remarkably similar properties to benzene. This molecule, which we call *borozone* for brevity, is planar, possesses a large first excitation energy, exhibits a highly aromatic character, and similar to benzene is a building block of possibly much larger aromatic compounds.

Small all-boron clusters,  $B_n$  ( $n < 20$ ) have been widely investigated both experimentally and theoretically [4–9]. All these studies indicate that small boron clusters assume in most cases quasi-planar structures and in some special cases even perfectly planar structures. In contrast, neutral and anionic boron hydrides,  $B_nH_{n+m}$ , are all known to have three-dimensional deltahedral structures [10]. There is yet little known about the structure of small boron hydrides where the number of hydrogen atoms is smaller than the number of boron atoms (see ref. [11] and references therein). One such example is the recently studied  $\sigma$ -aromatic and  $\pi$ -antiaromatic  $B_7H_2^-$  cluster, which is fully planar [11].

It was experimentally established that one of the most stable all-boron clusters is made up of twelve boron atoms, is quasi-planar in shape, and possesses a large first excitation energy of 2.0 eV [4]. The  $B_{12}$  structure consists of 13  $B_3$  triangles with 12 outer triangles surrounding a central one; the atoms forming the central triangle are situated above a nine-member boron ring making  $B_{12}$  a convex structure of  $C_{3v}$  symmetry [4–6, 9]. Our calculations revealed that the  $B_{12}$  cluster has three outer boron pairs that are 5% shorter than the average B–B bond lengths between the rest of the boron atoms. This suggests the presence of strong covalent bonds between those atoms. However, it is

N. G. Szwacki · C. J. Tymczak (✉)  
Department of Physics, Texas Southern University,  
Houston, TX 77004, USA  
e-mail: tymczakcj@tsu.edu

V. Weber  
Department of Physical Chemistry, University of Zurich,  
8057 Zurich, Switzerland

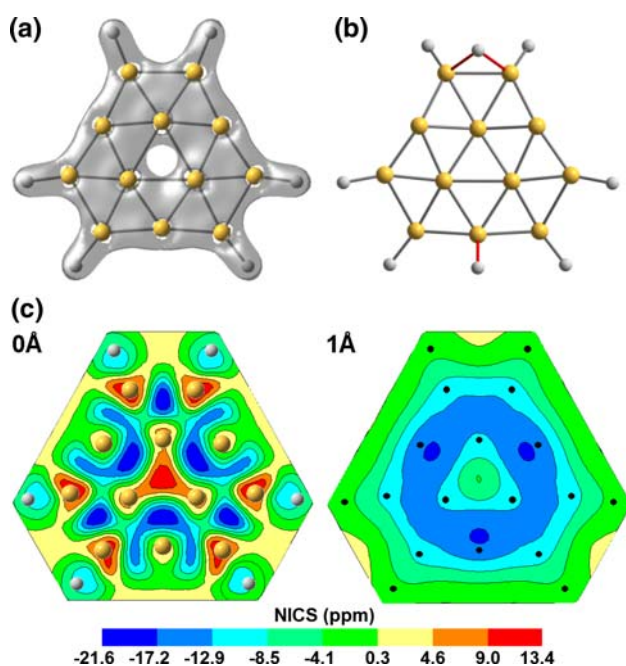


**Fig. 1** **a** Plot of the structures and total electronic densities of B<sub>12</sub>H<sub>6</sub>. Note that the density of electrons is weaker at the center of the “boron ring.” **b** Quasi-planar C<sub>s</sub> structure of B<sub>12</sub>H<sub>8</sub>, which is the energetically preferred configuration for B<sub>12</sub> with 4 H<sub>2</sub> molecules, attached to it. **c** A contour plot of NICS(*x*, *y*) for B<sub>12</sub>H<sub>6</sub> in plane (*left*) and at 1 Å above the planar molecule (*right*)

possible to increase the B–B bond lengths of the three outer pairs by 17% by attaching hydrogen atoms to the outer boron atoms (see Fig. 1a). The unexpected consequence of this is that the molecule becomes perfectly planar. This finding motivated us to investigate the interaction between B<sub>12</sub> cluster and up to four hydrogen molecules.

### Computational Details

The structure and electronic properties of all clusters were obtained at the X3LYP/6-311G(d,p) level of theory using tight convergence criteria as implemented in FreeON (formerly known as MondoSCF), a suite of programs using Gaussian basis sets and all-electron Hartree–Fock, density functional theory or hybrid approach for self-consistent electronic structure calculations [12–17]. The initial search for the most stable structures of the boron hydride B<sub>12</sub>H<sub>*n*</sub> have been done at the X3LYP/6-31G(d,p) level of theory starting from the energy-minimum structure of B<sub>12</sub>H<sub>*n-2*</sub> and the low-lying isomers in each case have been reoptimized using the 6-311G(d,p) basis set. The obtained local energy-minimum structures are well separated in energy from its higher isomers by at least 22 kcal/mol in the case of B<sub>12</sub>H<sub>*n*</sub>, where *n* ≤ 6, and 17 kcal/mol in the case of the B<sub>12</sub>H<sub>8</sub>

cluster. The B<sub>22</sub>H<sub>8</sub> and B<sub>60</sub>H<sub>12</sub> clusters, which result from the fusion of two and six B<sub>12</sub>H<sub>6</sub> molecules, respectively, were fully optimized using symmetry-unrestricted calculations.

To ensure that the structures for the neutral and negatively charged B<sub>12</sub>H<sub>6</sub> molecules correspond to a local minima of energy, the nature of the stationary points were checked by vibrational frequency calculations. In addition, several tests have been done for neutral B<sub>12</sub>H<sub>6</sub> optimizing this molecule starting from structures with randomly displaced atoms. For all tested cases, the substructure of boron atoms became planar after optimization to within 0.012 and 0.014 Å at the X3LYP/6-311++G(d,p) and UHF-MP2/6-311++G(d,p) levels of theory, respectively. Precise calculations at the X3LYP/6-311G(d,p) level of theory and using very tight convergence criteria reveal, however, that the fully planar B<sub>12</sub>H<sub>6</sub> molecule is the most energetically favorable structure. Similar tests were done for B<sub>22</sub>H<sub>8</sub> and B<sub>60</sub>H<sub>12</sub>, and after optimization at the X3LYP/6-311G(d,p) level of theory both substructures of boron atoms became planar to within 0.016 Å.

The first singlet excitation energy, nuclear magnetic resonance (NMR) shielding tensors, and magnetic susceptibility tensors were calculated using the Gaussian03 package [18]. This package was also used to further optimize the B<sub>12</sub>H<sub>6</sub> molecule using the 6-311++G(d,p) basis set. To obtain the nucleus independent chemical shift (NICS) values (from the NMR shielding tensors), we have used the GIAO (gauge-independent atomic orbital) method and the magnetic susceptibility tensors were calculated using the CSGT (continuous set of gauge transformations) method. All computations have been performed at the X3LYP/6-311++G(d,p) level of theory except for the B<sub>60</sub>H<sub>12</sub> cluster, for which we have used the RHF/6-31G(d,p) level of theory. The anisotropy of magnetic susceptibility is defined as the difference between out-of-plane and the average in-plane components of the susceptibility tensor.

The MOs of B<sub>12</sub>H<sub>6</sub> and C<sub>6</sub>H<sub>6</sub> were calculated at the RHF/6-311++G(d,p) level of theory using the GAMESS-US package [19]. The same package was used to calculate the π–π interaction between molecules in borozene and benzene dimmers at the RHF-MP2/6-311G(d,p) and RHF-MP2/6-311++G(d,p) levels of theory, respectively. The counterpoise correction was applied to account for the basis set superposition error.

### Results and Discussion

The search for the stable structures of B<sub>12</sub>H<sub>*n*</sub>, with *n* ≤ 6 is simplified by the fact that the most energetically favorable configurations, as far as we can determine, are those where the hydrogen atoms are directly attached to the outer boron

atoms of the molecule. We have established that the most likely stable configuration for  $B_{12}H_2$  is when the hydrogen atoms are attached to one of the outer short-bonded boron pairs of the  $B_{12}$  cluster. The energetically preferred configuration for  $B_{12}H_4$  is when the hydrogen atoms are attached to one of the two remaining outer short-bonded boron pairs in the  $B_{12}H_2$ . Finally, the  $B_{12}H_6$  cluster has all short B–B pairs, from  $B_{12}$ , with hydrogen atoms attached to them. Only  $B_{12}H_6$  is a fully planar molecule, whereas  $B_{12}H_2$  and  $B_{12}H_4$  are quasi-planar with  $C_s$  symmetry. In Fig. 1a, we have shown the structure of  $B_{12}H_6$ . The hydrogenation energy, defined as  $\Delta E = E(B_{12}H_n) - E(B_{12}H_{n-2}) - E(H_2)$  where  $E$  is the total energy, is  $-44$  kcal/mol for  $n = 2$ ,  $-45$  kcal/mol for  $n = 4$ , and  $-51$  kcal/mol for  $n = 6$ . We have found, however, that if a fourth  $H_2$  molecule is attached to  $B_{12}H_6$  the hydrogenation energy increases to  $-2$  kcal/mol (i.e., the  $H_2$  molecule is weakly bound to  $B_{12}H_6$ ). It is also important to mention that our  $\Delta E$  values are about two times larger than the predicted energy of hydrogenation of the  $B_7^-$  cluster [11], which is an additional indication of unusual stability of the  $B_{12}$  structure. The  $B_{12}H_8$  molecule is shown in Fig. 1b and can be described as a distorted  $B_{12}H_6$  cluster with two extra (one terminal and one bridging) hydrogen atoms attached to it. The B–H bond lengths are 1.36 and 1.21 Å for the bridging and terminal hydrogen atoms, respectively, whereas the remaining B–H distances in  $B_{12}H_8$  and in all other described earlier  $B_{12}H_n$  ( $n \leq 6$ ) clusters are the same and equal to 1.18 Å. The last value is very close to the calculated bond lengths B–H = 1.19 Å in borane,  $BH_3$ .

Although no single measure of aromaticity is without limitations, the anisotropy of the magnetic susceptibility (AMS) is an important indicator of diatropicity [20]. The  $B_{12}H_6$  molecule has very important properties: it is planar with  $D_{3h}$  symmetry; it possesses a large first excitation energy of 2.6 eV and a large AMS of  $-208.2$  cgs-ppm. Also, the  $B_{12}H_6$  molecule can be a building block of larger planar molecules with similar structural and physical characteristics. In Fig. 2a, b are shown what we call boron analogs of naphthalene ( $B_{22}H_8$ ) and coronene ( $B_{60}H_{12}$ ), which are fusions of two and six  $B_{12}H_6$  clusters, respectively (It should be pointed out that the idea of boron analogs of both benzene and naphthalene are not new, since the all-boron  $B_{12}$  molecule was previously indicated [4] to be an analog of benzene and very recently also an all-boron analog of naphthalene was proposed [7]). Also of interest, the HOMO–LUMO (HOMO, highest occupied molecular orbital; LUMO, lowest unoccupied molecular orbital) gap decreases with cluster size. The gap values are 3.6, 2.4, 1.3 eV for  $B_{12}H_6$ ,  $B_{22}H_8$ ,  $B_{60}H_{12}$ , respectively. Furthermore, the absolute AMS value increases with cluster size; the AMS values are  $-294.3$ ,  $-454.7$  for  $B_{22}H_8$ ,  $B_{60}H_{12}$ , respectively. This and other values for the

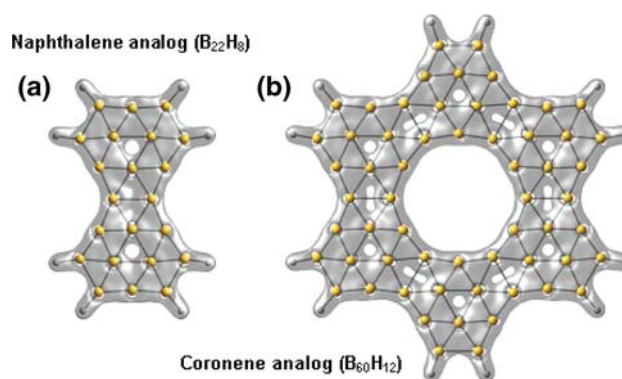


**Fig. 2** Plot of the structures and total electronic densities of **a**  $B_{22}H_8$ , and **b**  $B_{60}H_{12}$ . In both molecules, all B–H distances are the same and equal to 1.18 Å

studied boron hydrides are summarized in Table 1. In this table, we have also included the calculated values for  $B_{12}$  with enforced planarity ( $D_{3h}$ ) and the fully relaxed structure ( $C_{3v}$ ). We have in addition included the values for three hydrocarbons for comparison. It should be noted that the absolute value of AMS for  $B_{12}H_6$  is three times larger than our value for benzene ( $-67.5$  cgs-ppm) and 7% larger than the value for the  $C_{3v}$   $B_{12}$  cluster ( $-192.9$  cgs-ppm).

To gain information about the individual contributions of the  $B_3$  triangles to the overall aromaticity of the  $B_{12}H_6$  molecule, we have studied its two-dimensional NICS map. In Fig. 1c, we have shown the contour plot of NICS(x, y) in plane (left) and at 1 Å above the  $B_{12}H_6$  molecule (right). It is clearly seen from the left part of the figure that the NICS values are negative inside the twelve outer  $B_3$  triangles of the molecule, suggesting a flow of a global diatropic current around the central triangle. The central part of the molecule has a paratropic current flowing inside the inner  $B_3$  triangle which is not overwhelmed by a diatropic current due to an electron charge transfer from the center of

**Table 1** Molecular symmetry, HOMO–LUMO energy gaps, and the isotropic and anisotropic values of magnetic susceptibility for the studied planar boranes and hydrocarbons

Structure	Symmetry	HOMO–LUMO gap (eV)	Magnetic susceptibility (cgs-ppm)	
			Isotropy	Anisotropy
$B_{12}$	$C_{3v}$	3.73	$-105.4$	$-192.9$
$B_{12}$	$D_{3h}$	3.58	$-107.6$	$-213.6$
$B_{12}H_6$	$D_{3h}$	3.67	$-92.0$	$-208.2$
$B_{22}H_8$	$D_{2h}$	2.38	$-147.9$	$-294.3$
$B_{60}H_{12}$	$D_{6h}$	1.30	$-286.5$	$-454.7$
$C_6H_6$	$D_{6h}$	6.86	$-53.0$	$-67.5$
$C_{10}H_8$	$D_{2h}$	4.93	$-90.4$	$-128.5$
$C_{24}H_{12}$	$D_{6h}$	4.13	$-251.1$	$-474.5$

For comparison, we have also included our results for  $B_{12}$  with enforced planarity ( $D_{3h}$ ) and the fully relaxed structure ( $C_{3v}$ )

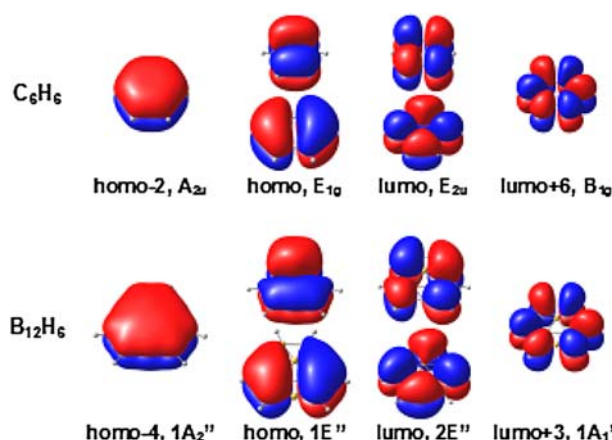


**Fig. 3** Comparison of the  $\pi$  molecular orbitals of benzene with the corresponding  $\pi$  molecular orbitals of  $B_{12}H_6$

the structure towards the outer boron triangles after hydrogenation. Also, this antiaromatic region is spatially localized since the NICS values are negative at 1 Å (see the right part of Fig. 1c) and 2 Å above and below the center of the  $B_{12}H_6$  molecule (NICS(1) = −3.9 ppm; NICS(2) = −5.2 ppm).

The benzene dimer is the simplest prototype of the aromatic  $\pi$ – $\pi$  interactions which is an important weak interaction present in aromatic supramolecular systems [12]. Since the number of  $\pi$  electrons in borozene and benzene is the same and the molecular orbital (MO) picture for these electors is very similar (see Fig. 3), we may expect that the strength of the aromatic–aromatic interaction in a borozene dimer is comparable to that of the benzene dimer. To investigate this, we have considered the simplest case where the molecules in the dimer have the parallel “sandwich” configuration. In Fig. 4, we plotted the association energy versus the distance between the molecules in the  $B_{12}H_6$  and  $C_6H_6$  dimmers. From this figure, we can see that the association energy for the borozene dimer, in its equilibrium position, is about five times larger than the corresponding energy for the benzene dimer. This result suggests a stronger polarization contribution from borozene’s  $\pi$ -MOs, which we theorize is a consequence of more delocalized  $\pi$ -electrons in the borozene dimer with respect to the benzene dimer.

Finally, we have also calculated the electron affinity (EA) and the ionization energy (IE) for  $B_{12}H_6$ . The values are summarized in Table 2 calculated at two levels of theory. The agreement between the values obtained using the hybrid functional and MP2 is quite good. The EA values are positive what means that the  $B_{12}H_6^-$  molecule is stable with respect to  $B_{12}H_6$  and a free electron. However, an addition of an electron to  $B_{12}H_6$  costs energy since the EA is negative and large (see Table 2). A removal of one electron from  $B_{12}H_6$  costs a lot of energy since the vertical IE values are very large: 8.52 and 8.72 eV for X3LYP and

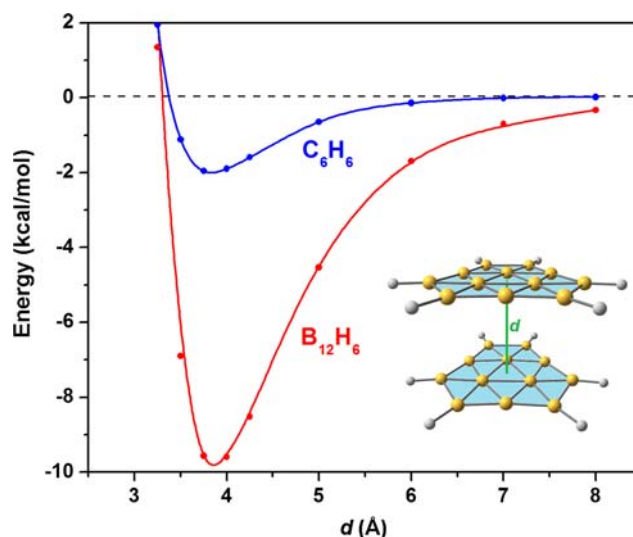


**Fig. 4** Potential energy curves for  $B_{12}H_6$  and benzene dimers versus the center-to-center distance between the monomers. The association energies are −1.99 and −9.81 kcal/mol and the equilibrium distances are 3.8 and 3.9 Å for  $C_6H_6$  and  $B_{12}H_6$ , respectively

**Table 2** Vertical electron affinities and ionization energies for  $B_{12}H_6$  and  $B_{12}H_6^-$  calculated using the 6-311++G(d,p) basis set

	Electron affinity (eV)		Ionization energy (eV)	
	$B_{12}H_6$	$B_{12}H_6^-$	$B_{12}H_6$	$B_{12}H_6^-$
X3LYP	1.69 (1.80)	−2.57	8.52	1.97 (1.80)
UHF-MP2	1.52 (1.71)	−2.18	8.72	1.89 (1.71)

The numbers in brackets correspond to the adiabatic values for EA and IE. All values have been obtained from differences in total energies

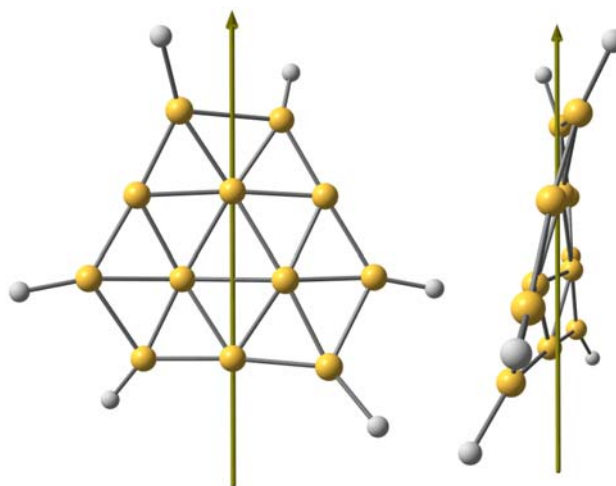


**Fig. 5** Front (left) and side (right) views of the negatively charged  $B_{12}H_6$  molecule. The  $C_2$  rotation axis is shown



MP2, respectively. The structure of  $B_{12}H_6^-$  is shown in Fig. 5. This molecule has  $C_2$  symmetry and the axis of rotation is shown in the figure. The  $D_{3h}$  symmetry of  $B_{12}H_6$  is reduced here to  $C_2$  since the charged molecule is “twisted” along the shown axis.

Although the specific route for the synthesis of the  $B_{12}H_6$  (or  $B_{12}H_6^-$ ) structure is not yet known, it is clear from our investigation that to some extent the chemistries of  $B_{12}H_6$  and benzene may be very similar, suggesting that similar methods could be employed to synthesize this and related compounds. Given the technological importance of benzene and its derivatives, we believe that the  $B_{12}H_6$  molecule will have a significant technological impact and deserves further extensive study.

**Acknowledgments** We would like to thank Dr. Daniel Vrinceanu for his helpful discussion and Brad Mazock for computational support. This project was supported by the Robert A. Welch Foundation (Grant J-1675) and the NIH-RCMI Program (Grant RR03045).

## References

1. D. Lloyd, J. Chem. Inf. Comput. Sci. **36**, 442 (1996). doi:10.1021/ci950158g
2. P.v.R. Schleyer, H. Jiao, Pure Appl. Chem. **68**, 209 (1996). doi:10.1351/pac199668020209
3. X. Li, A.E. Kuznetsov, H.-F. Zhang, A.I. Boldyrev, L.-S. Wang, Science **291**, 859 (2001). doi:10.1126/science.291.5505.859
4. H.-J. Zhai, B. Kiran, J. Li, L.-S. Wang, Nat. Mater. **2**, 827 (2003). doi:10.1038/nmat1012
5. D.Y. Zubarev, A.I. Boldyrev, J. Comput. Chem. **28**, 251 (2007). doi:10.1002/jcc.20518
6. A.N. Alexandrova, A.I. Boldyrev, H.-J. Zhai, L.-S. Wang, Coord. Chem. Rev. **250**, 2811 (2006). doi:10.1016/j.ccr.2006.03.032
7. A.P. Sergeeva, D.Y. Zubarev, H.-J. Zhai, A.I. Boldyrev, L.-S. Wang, J. Am. Chem. Soc. **130**, 7244 (2008). doi:10.1021/ja802494z
8. J.-i. Aihara, H. Kanno, T. Ishida, J. Am. Chem. Soc. **127**, 13324 (2005). doi:10.1021/ja053171i
9. I. Boustani, Int. J. Quantum Chem. **52**, 1081 (1994). doi:10.1002/qua.560520432
10. W.N. Lipscomb, Inorg. Chem. **3**, 1683 (1964). doi:10.1021/ic50022a005
11. A.N. Alexandrova, E. Koyle, A.I. Boldyrev, J. Mol. Model. **12**, 569 (2006). doi:10.1007/s00894-005-0035-5
12. M.O. Sinnokrot, E.F. Valeev, C.D. Sherrill, J. Am. Chem. Soc. **124**, 10887 (2002). doi:10.1021/ja025896h
13. C.K. Gan, C.J. Tymczak, M. Challacombe, J. Chem. Phys. **121**, 6608 (2004). doi:10.1063/1.1790891
14. K. Németh, M. Challacombe, J. Chem. Phys. **121**, 2877 (2004). doi:10.1063/1.1771636
15. C.J. Tymczak, M. Challacombe, J. Chem. Phys. **122**, 134102 (2005). doi:10.1063/1.1853374
16. C.J. Tymczak, V.T. Weber, E. Schwegler, M. Challacombe, J. Chem. Phys. **122**, 124105 (2005). doi:10.1063/1.1869470
17. A.M.N. Niklasson, C.J. Tymczak, M. Challacombe, Phys. Rev. Lett. **97**, 123001 (2006). doi:10.1103/PhysRevLett.97.123001
18. M.J. Frisch, G.W. Trucks, H.B. Schlegel, G.E. Scuseria, M.A. Robb, J.R. Cheeseman, J.J.A. Montgomery, T. Vreven, K.N. Kudin, J.C. Burant, J.M. Millam, S.S. Iyengar, J. Tomasi, V. Barone, B. Mennucci, M. Cossi, G. Scalmani, N. Rega, G.A. Petersson, H. Nakatsuji, M. Hada, M. Ehara, K. Toyota, R. Fukuda, J. Hasegawa, M. Ishida, T. Nakajima, Y. Honda, O. Kitao, H. Nakai, M. Klene, X. Li, J.E. Knox, H.P. Hratchian, J.B. Cross, V. Bakken, C. Adamo, J. Jaramillo, R. Gomperts, R.E. Stratmann, O. Yazyev, A.J. Austin, R. Cammi, C. Pomelli, J.W. Ochterski, P.Y. Ayala, K. Morokuma, G.A. Voth, P. Salvador, J.J. Dannenberg, V.G. Zakrzewski, S. Dapprich, A.D. Daniels, M.C. Strain, O. Farkas, D.K. Malick, A.D. Rabuck, K. Raghavachari, J.B. Foresman, J.V. Ortiz, Q. Cui, A.G. Baboul, S. Clifford, J. Cioslowski, B.B. Stefanov, G. Liu, A. Liashenko, P. Piskorz, I. Komaromi, R.L. Martin, D.J. Fox, T. Keith, M.A. Al-Laham, C.Y. Peng, A. Nanayakkara, M. Challacombe, P.M.W. Gill, B. Johnson, W. Chen, M.W. Wong, C. Gonzalez, J.A. Pople, Gaussian 03, Revision E.01 (Gaussian, Wallingford, 2004)
19. M.W. Schmidt, K.K. Baldridge, J.A. Boatz, S.T. Elbert, M.S. Gordon, J.H. Jensen, S. Koseki, N. Matsunaga, K.A. Nguyen, S. Su, T.L. Windus, M. Dupuis Jr., J. AM, J. Comput. Chem. **14**, 1347 (1993). doi:10.1002/jcc.540141112
20. P. Lazzeretti, Phys. Chem. Chem. Phys. **6**, 217 (2004). doi:10.1039/b311178d